Anti-icing Behavior of Thermally Sprayed Polymer Coatings

Anti-Icing Behavior of Thermally Sprayed Polymer Coatings

Heli Koivuluoto, Christian Stenroos, Mikko Kylmälahti, Marian Apostol, Jarkko Kiilakoski, Petri Vuoristo
Tampere University of Technology, Department of Materials Science, Korkeakoulunkatu 6, 33720 Tampere, Finland

Keywords: Anti-icing, flame spraying, polymer coatings, wear behavior

Abstract

Surface engineering shows an increasing potential to provide a sustainable approach to icing problems. Currently, several passive anti-ice properties adoptable to coatings are known, but further research is required to proceed for practical applications. This is due to the fact that icing reduces safety, operational tempo, productivity and reliability of logistics, industry and infrastructure. An icing wind tunnel and a centrifugal ice adhesion test equipment can be used to evaluate and develop anti-icing and icephobic coatings for a potential use in various arctic environments, e.g. in wind power generation, oil drilling, mining and in logistic industries. The present study deals with evaluation of icing properties of flame-sprayed polyethylene (PE) -based polymer coatings. In the laboratory-scale icing tests, thermally sprayed polymer coatings showed low ice adhesion compared with metals such as aluminum and stainless steel. The ice adhesion strength of the flame-sprayed PE coating was found to have approximately seven times lower ice adhesion values compared with metallic aluminum, indicating a very promising anti-icing behavior.

1. Introduction

On-going climate change, opening of new logistic routes, energy and mineral resources as well as increasing tourism feed the growing activity in cold climate regions. One of the major challenges for operations in these areas is ice and snow accretion. Icing reduces safety, operational tempo, productivity and reliability of logistics, industry and infrastructure. Atmospheric icing on the surfaces is a very complex phenomenon and multiple factors affect the accretion process and behavior of ice on the surface. (Ref. 1) From a climatic point of view, several basic processes influence greatly the severity of icing, accretion rate and ice type. These are water cycle, wind speed, the formation of clouds,

precipitation and presence of different phases (vapor, liquid, and solid) of atmospheric water. (Refs. 2-4) Several factors affect the ice accretion and ice adhesion. For instance, surface topography, surface chemistry and wetting behavior, as well as ice characteristics (type, temperature and liquid water content) have been reported having an influence on ice adhesion, indicating the complexity of icing on surfaces. (Refs. 5-8)

Surface engineering has high potential as a sustainable approach in solving icing problems. Passive anti-ice coatings can hinder ice formation and icephobic surfaces can reduce the adhesion of ice to surfaces. At this moment, current commercial coatings with icephobic characteristics rely often on hydrophobicity, releasing of lubricants or melting point depressants and ablation. Research is additionally carried out on icephobic potential of superhydrophobic surfaces (Ref. 9), phase change materials (Ref. 10), slippery liquid infused surfaces (Ref. 11) and surface morphology (Refs. 9,12). All these anti-ice mechanisms show promising results in reducing ice accretion and adhesion. Nevertheless, so far they are functional only in specific icing conditions for a very limited length of time. Moreover, the wear resistance of these coatings is known to be poor and therefore, the current coatings are practical only in limited applications or the icephobic effect is significantly insufficient (Ref. 13).

Generally, coatings have been presented to offer an environmentally friendly option because no external energy is needed to remove ice and coatings can be tailored to be free of harmful chemicals. Different coating strategies have been presented which can be roughly divided into polymeric coatings containing fluorine or silicone compounds and superhydrophobic polymer composite coatings. Their performance as icephobic coatings is based on the hydrophobicity, which is achieved by proper surface chemistry and roughness. In addition to the low-ice-adhesion surfaces, the future aim is to be able to prevent ice formation on the structures. (Ref. 1)

At this moment, studies related to the icing behavior of thermally sprayed polymer coatings are not available in literature. However, flame spraying is one of the common thermal spray methods for spraying polymer coatings (Refs. 14,15) and therefore, it is interesting to study the icing behavior of these polymer coatings. In flame spraying of polymers, the material is fed in the form of powder to the flame formed by e.g., the mixture of oxygen-acetylene. The powder melts in the flame and molten

droplets are spread on the sprayed surface. Advantages of thermally sprayed polymer coatings are related to the low cost and high performance of the coatings (Refs. 15,16).

Flame-sprayed polyethylene (PE) coatings have previously been studied by Vuoristo et al. (Ref. 17). The research focused on the use of flame-sprayed PE coatings as natural gas pipe-line coatings. On the other hand, ultra-high molecular weight polyethylene (UHMWPE) is known to have good protective properties and flame-sprayed UHMWPE coatings have also been studied elsewhere (Ref. 18). Flame-sprayed PE coatings have primary applications in corrosion protection of components and metal structures instead of paints and metallic coatings. Moreover, they can be used in other applications such as friction lowering, non-stick surfaces, decoration, etc. One benefit is also their applicability in difficult processing conditions. (Ref. 14) Additionally, thermally sprayed fluoropolymer coatings have shown good corrosion properties (Ref. 19).

This research focuses on the icing behavior of flame-sprayed PE-based coatings. Icephobic coatings have high potential to protect metal surfaces e.g., aluminum which is not an ideal icephobic material because it has a high surface energy value (Ref. 20). The aim of this study is to evaluate ice adhesion, wetting behavior, surface roughness, erosion and impact behavior of flame-sprayed PE-based coatings and reference materials such as aluminum, stainless steel and polyurethane paint.

2. Experimental Procedure

Polymer coatings were sprayed using an oxygen-acetylene flame spray gun (Castodyn DS 8000, Castolin Eutectic, Switzerland). Gas pressures were 400 kPa (oxygen) and 70 kPa (acetylene). Powder was fed by a powder feeder (Sulzer Metco 4MP, Switzerland) using air as a carrier gas. Gas flows were set relatively low in order to prevent overheating and burning of the powder by the flame. Prior to spraying the samples were cleaned with alcohol. After spraying, a few re-melting passes were done without feeding powder in order to densify the structure. Commercially available and thermally sprayable polyethylene (PE, particle size 230 µm and melting point 128°C) and ultra-high molecular weight polyethylene (UHMWPE, particle size 30 µm and melting point 136°C) powders were used in the experiments. In addition, fine fluoropolymer perfluoroethylene-propylene (FEP, particle size 22 µm and melting point 260 - 290°C) powder was mixed with PE powder (10, 25 and 50 wt.%). Substrate

material was stainless steel. Reference surfaces were polished stainless steel, polished aluminum and commercial two-component polyurethane (PU) paint (BladeRep LEP 9). The as-received stainless steel was mirror-polished (Sa=0.230 µm) whereas the aluminum reference surface was fine-grinded till 4000 grit SiC-paper and mirror-polished with 1 µm diamond polishing (Sa=0.255 µm).

For the icing research, a novel icing wind tunnel was used in order to create artificial ice, which correspond outdoor icing conditions. The wind tunnel is placed in a cold climate room where the temperature can be varied from room temperature to –40ºC. After ice accretion, the ice adhesion was measured with a centrifugal ice adhesion test, placed also in cold climate room (Refs. 1,21). Figure 1 presents the ice testing rig located in Tampere University of Technology (TUT).

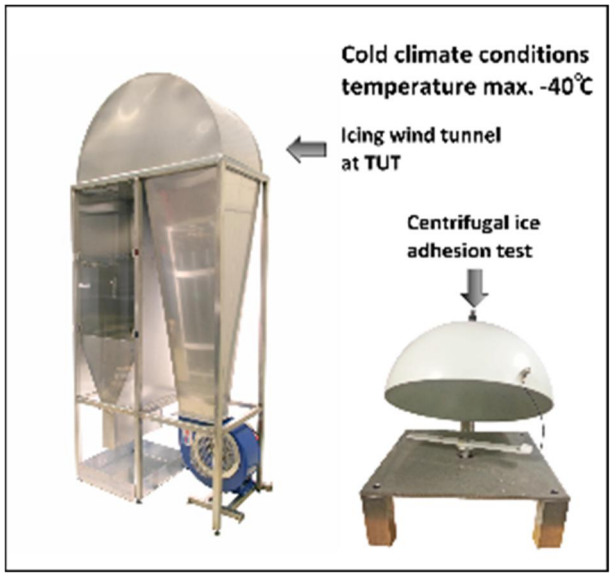

Figure 1. Icing wind tunnel and centrifugal ice adhesion test at TUT. Modified from (Refs. 1,21).

In a centrifugal ice adhesion test, the ice-accreted samples are rotated with the constant acceleration until the ice block detaches. The detachment is observed with acceleration sensor, which is attached into the protective dome around blade. The samples are attached into the blades with screws and the blades are balanced to minimize vibration and stress for the servo motor and its axis. The equipment is based on the equipment described by Laforte and Beisswenger (Ref. 22). When adhesion area is measured and the speed of rotation at the moment of detachment are known, the maximum adhesive shear strength can be calculated. The centrifugal force *F* [N] can be written as shown in Equation 1:

$$F = mr\omega^2 \qquad \text{(Eq. 1)}$$

Where *m* [kg] is the mass, *r* [m] is the radius of rotation and *ω* [rad/s] is angular velocity. By measuring rpm value at the moment of ice release, angular velocity can be calculated. The mass of ice block is measured by weighing the sample before and after the ice detachment. The radius of the rotation is 17 cm, which is kept constant. The shear stress *τ* [Pa] can calculated with the Equation 2:

$$\tau = \frac{F}{A} \qquad \text{(Eq. 2)}$$

Where *F* [N] is centrifugal force and *A* [m^2] is the contact area of the detached ice. After the ice detachment, the contact area of the accreted ice block can be measured. By dividing the centrifugal force with the contact area, the ice adhesion shear strength can be calculated.

The temperature was chosen as –10 ºC and the air flow velocity was set to the maximum 25 m/s. The mixed ice was accreted from supercooled water droplets, which volume median diameter is 31 µm. The droplet sizes are given based on nozzle manufacturer data. Different ice types e.g., rime, glaze and the mixture of those can be created in the icing wind tunnel, Fig. 2. More details of ice adhesion measurements can be found in the previous studies (Refs. 1,21). Ice adhesion was measured as an average of four measurements. An effect of surface quality on the ice adhesion was studied by measuring the ice adhesions of the coatings in as-sprayed and polished states.

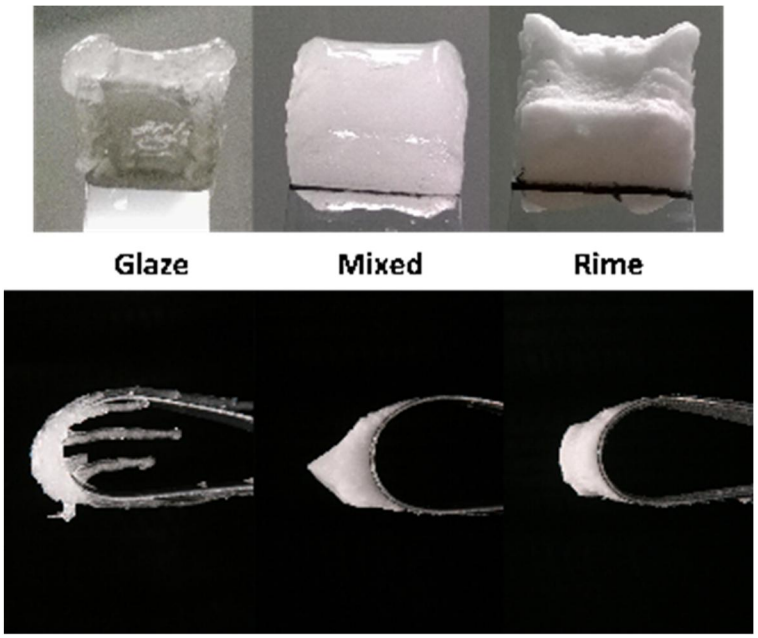

Figure 2. Different ice types formed in the icing wind tunnel. Glaze ice, rime ice and mixture of them (mixed ice) on steel plates and aerodynamic profiles. Modified from (Ref. 1).

Contact angle (CA) measurements were carried out by using distilled water and KSV CAM200 equipment (KSV Instruments Oy, Finland). The measurements were performed in a controlled environment, where relative humidity was 50 % and temperature 23°C. A droplet volume of 5 µl was used for static contact angle measurements. At least five droplets were used for determining the static contact angle.

Surface properties (surface profile and Sa-values) were analyzed by an optical profilometer (Alicona Infinite Focus G5, Alicona Imaging GmbH, Germany). Sa-values were measured from areas as large as possible in order to properly assess the surface roughness. In addition, volume losses and impact areas are determined after high velocity impact test by the optical profilometer. Surface roughness (Ra-values) was measured before and after erosion tests with a surface roughness tester (Mitutoyo SJ-301, Japan).

Dry particle erosion wear behavior of the coatings was studied with a centrifugal erosion tester (Erosion test 1). This test was performed for the polished samples. Samples were attached in 90°-angle in the sample holders. Rotation speed was set to 6000 rpm, which corresponds to an impact velocity of 80 m/s for the abrasives. Samples were exposed to a total of 5 kg of dry quartz sand (SiO_2) with a grain size of 0.1–0.6 mm. In order to calculate mass loss, samples were weighed before and after tests.

The micro-sandblasting test (Erosion test 2) was conducted to assess the wear behavior of the flame-sprayed coatings. The distance between the abrasive gun and the sample was set to 30 mm. The exposed area of the sample was 25 mm in diameter. Sample surfaces were sand-blasted with Al_2O_3 abrasive (-340 +170 µm) at 2.5 bar pressure for 120 s. Mass losses and roughness changes were measured.

High velocity impact tests were conducted with the high velocity particle impactor at Tampere Wear Center (Tampere University of Technology, Department of Materials Science). The device used in these impact tests is presented in (Ref. 23). In the high velocity particle impactor, a single particle is fired with a smooth-bore compressed-air gun towards the sample. In order to determine the initial kinetic energy prior to the impact, the incident velocity was measured with a commercial chronometer (ProChrono

digital, Competition Electronics, USA) placed in front of the target assembly. The impact event was recorded with a high speed camera (NAC, Memrecam fx K5, NAC Image Technology, USA), in order to calculate residual kinetic energy with image analysis. (Refs. 23-27) Based on high-speed images from the impact event, the dissipated energy E_d [J] of the projectile can be calculated by comparing the initial and post-impact kinetic energies of the projectile. The dissipated energy of the projectile is described with Equation 3.

$$E_d = \frac{1}{2} m_p \left(v_i - \frac{\Delta s}{\Delta t} \right)^2 \qquad \text{(Eq. 3)}$$

where m_p [kg], v_i [m/s], Δs [m], Δt [s] are the projectile's mass and initial velocity, displacement of a sample point between two images and the time consumed for this displacement of the projectile. With the custom image-analysis suite, the velocity of the rebounded projectiles after the impacts was assessed by overlaying two post-impact images where the rebounded projectile is no longer in contact with the sample. (Refs. 24,25,28)

High velocity impact tests were performed in room temperature (22 °C) and at -10 °C. Samples were attached to the sample holder at a 60 degree angle with respect to the impact angle of the projectile. 5 mm carbon steel balls (Spherotech, CHR-005, 0.51 g) were used as projectiles whose velocities were 50±1 m/s. Initial kinetic energy of the impact was 0.64±0.03 J. Cooling of the impact-test samples at -10 °C was performed with a specific cooling system, where liquid nitrogen was carried with nitrogen gas to the target assembly. K-type thermocouples were attached on the sample surfaces in order to monitor and control the temperature of the samples. To guarantee sufficient cooling of the coating and the substrate, samples were kept at -12 °C for 10 min. After the cooling of the samples, cooling box was removed and projectile was shot, when the temperature of the sample was -10±0.5ºC. Cross-sections of impact craters were examined with a scanning electron microscope (SEM, Philips XL30, The Netherlands) in order to characterize possible subsurface cracks and to assess deformation of the surface. Coating structures were also studied with SEM.

3. Results and Discussion

3.1 Structure of Flame-Sprayed Polymer Coatings

Flame-sprayed PE and PE+FEP coatings possess dense structures, Fig. 3. Similarly, dense thermally sprayed fluoropolymer coatings were reported by Leivo et al. (Ref. 19). In Fig. 3a, the homogeneous

structure of flame-sprayed PE coating is presented. Some pores or gas-pockets were detected close to the coating surface, Fig. 3b. Flame-sprayed PE+25%FEP coatings are presented in Fig. 3c and 3d. FEP distribution in flame-sprayed PE+25FEP coatings seem to be relatively randomly distributed in PE-matrix as showed in Fig. 3c and Fig. 3d. More even distribution of FEP particles might have been achieved if the particle size distributions of the PE and FEP powders would have been closer to each other. The FEP powder used in this study was very fine. Defect-free and poreless polymer coatings can be produced by thermal spraying with optimized process parameters and powders tailored for thermal spraying (Ref. 19).

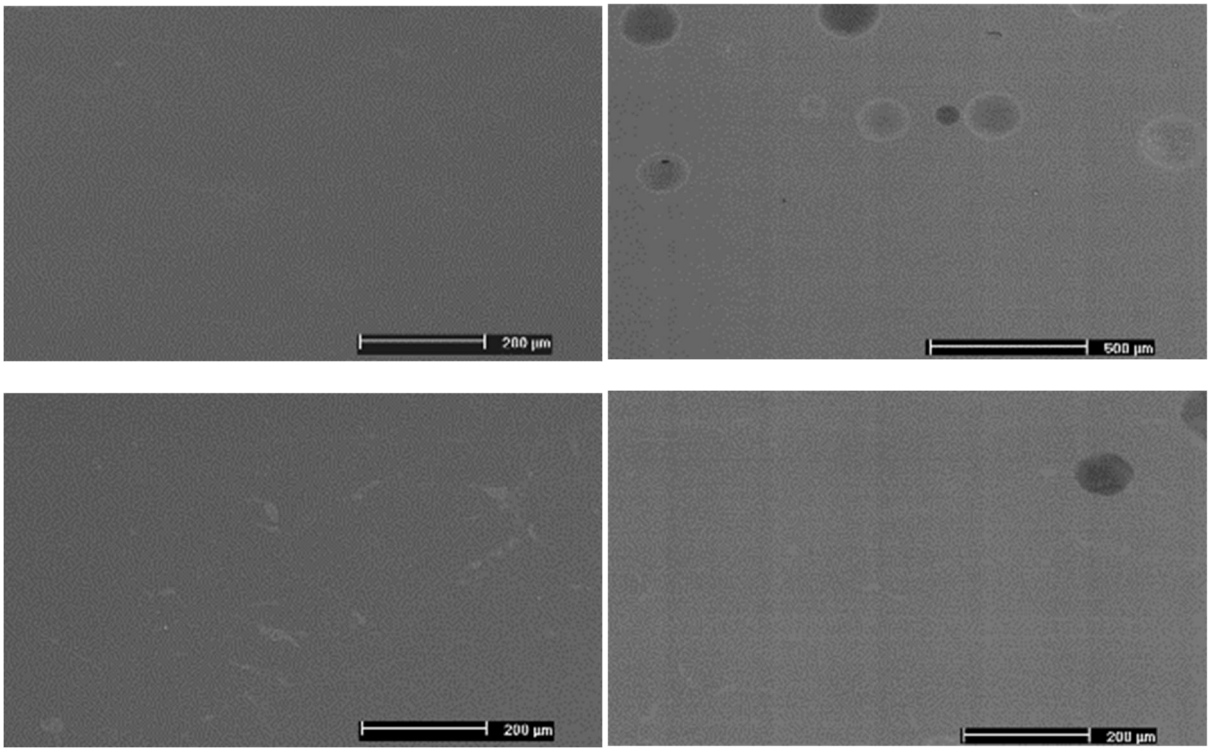

Figure 3. Cross sectional structures of flame-sprayed a) PE (SEM/SE image) and b) PE (SEM/BSE image), c) PE+FEP (SEM/SE image) and d) PE+FEP (SEM/BSE image) coatings.

3.1 Ice Adhesion of Flame-Sprayed Polymer Coatings

Ice adhesion values of the flame-sprayed PE-based coatings are presented in Fig. 4. Ice adhesion of flame-sprayed UHMWPE, PE and PE+25FEP coatings was measured in the as-sprayed state. Surface roughness plays a role in ice adhesion and therefore, surfaces were also polished in order to avoid /diminish the effect of surface roughness and focus on the effect of coating material itself. Flame-sprayed UHMWPE coating had higher ice adhesion with higher standard deviation compared with

flame-sprayed PE and PE+FEP coatings although it was smoother in the as-sprayed state (Table 1). The general finding is that ice adhesion increases as the surface roughness increases (Refs. 20,29,30) which is also seen here in the comparison between the as-sprayed and polished coating surfaces. Polished flame-sprayed PE-based coatings had similar ice adhesion values, around 54 kPa, indicating good icing behavior. In this study, FEP increment in the powder did not affect the ice adhesion much due to the low amount of FEP in the coating structure in all cases.

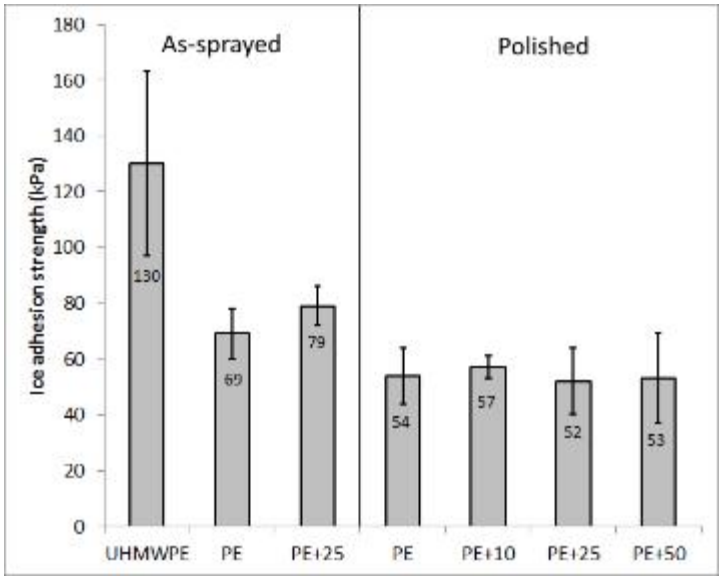

Figure 4. Ice adhesion strengths (and standard deviations) of as-sprayed and polished flame-sprayed PE-based coatings.

Table 1. Contact angle (CA), surface roughness (Sa) and ice adhesion of flame-sprayed PE-based coatings (as-sprayed and polished), reference metals and PU-paint.

Sample	Contact angle, CA (°)	Surface roughness, Sa (µm)	Ice adhesion (kPa)
FS UHMWPE (As-sprayed)	91	1.65	130
FS PE (As-sprayed)	79	2.05	69
FS PE+25 (As-sprayed)	85	5.44	79
FS PE (Polished)	97	0.64	54
FS PE+10 (Polished)	92	0.75	57
FS PE+25 (Polished)	91	1.13	52
FS PE+50 (Polished)	88	0.96	53
Stainless steel (SS, Polished)	61	0.23	269
Aluminum (Al, Polished)	66	0.26	380
PU-paint	79	2.24	82

Anti-icing behavior of polished flame-sprayed PE-coatings was compared with the behavior of metal sheets, such as stainless steel and aluminum plates, and reference PU-paint. Ice adhesions of these surfaces are presented in Fig. 5. Ice adhesion of flame-sprayed PE-coating was the lowest in this comparison. It was five times lower than the ice adhesion of stainless steel plate, seven times lower than the ice adhesion of aluminum plate and 1.5 times lower than the ice adhesion of PU-paint. PU-paint had the second lowest ice adhesion in this study (3.3 times lower than stainless steel and 4.6 times lower than aluminum).

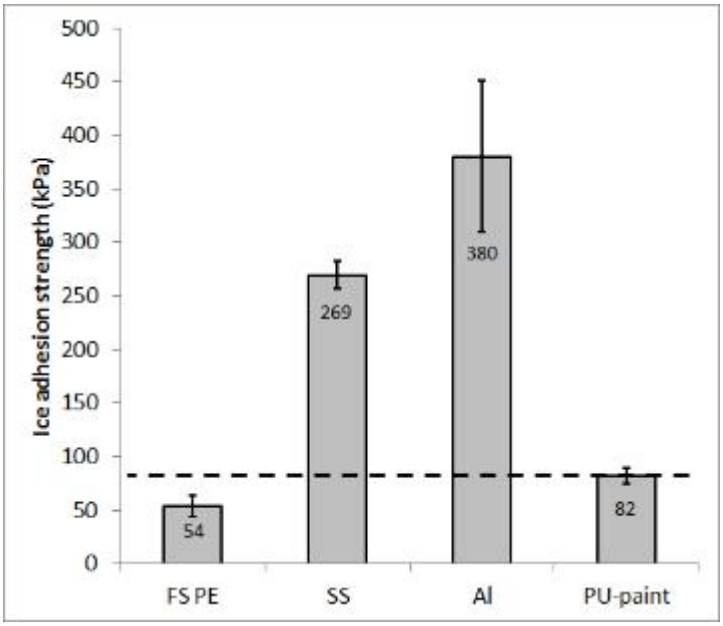

Figure 5. Ice adhesion strengths (and standard deviations) of flame-sprayed PE (FS PE) coating, stainless steel (SS) bulk material, aluminum (Al) bulk material and PU-paint.

3.2 Surface Properties of Flame-Sprayed Polymer Coatings

In addition to the surface roughness, wetting behavior has been reported to have a relation with the icing behavior of surfaces (Ref. 1). However, surface roughness has also a great impact on the wetting characteristics (Refs. 30,31), thereby these factors are connected to each other as well. Table 1 presents the contact angle, surface roughness and ice adhesion values of studied surfaces. Water contact angle values indicate the wetting behavior. Hydrophilic surfaces possess contact angles below 90°. This means that the water will wet the surface and penetrate the surface texture. When the water contact angle is over 90°, the surface is called hydrophobic. The wettability of the reference metal surfaces, stainless steel and aluminum, is hydrophilic. These surfaces are widely used in outdoor

applications so improving icephobicity is beneficial for these surfaces. Also the icing behavior of aluminum is widely studied in literature (Refs. 20,31-34). The polished flame-sprayed PE-based coatings were hydrophobic whereas the as-sprayed coatings were slightly hydrophilic due to the surface roughness.

It has been reported that different factors, such as surface roughness, wettability and surface energy, can have an influence on the ice adhesion strength (ice adhesion). For example, it has been proposed that increasing the water contact angle should decrease ice adhesion strength. The superhydrophobic surfaces have shown low ice adhesion values (Ref. 35), but their performance cannot be guaranteed due to the frost formation on the surfaces and a mechanical interlocking effect (Refs. 31,33,34). Therefore, durability of the anti-icing surfaces is also a very important issue.

3.3 Wear Behavior

3.3.1 Dry Particle Erosion

Flame-sprayed PE-based coatings have shown good anti-icing properties i.e. low ice adhesion values. In addition to that, the erosion behavior of the coatings was evaluated. Two erosion tests were used: dry particle erosion (traditional test for thermally sprayed coatings, Erosion test 1) and a micro-sandblasting test (modified for this study, Erosion test 2) in order to evaluate the coating performance and durability. Table 2 presents the erosion test results. PU-paints have low erosion resistance and they wore out during both erosion tests. In Erosion test 1, PU-paint wore out after 1 kg test (total 5 kg) and therefore, the second erosion test (micro-sandblasting) was used. In Erosion test 2, the erosive is smaller than in Erosion test 1 but still PU-paint surface eroded totally.

Table 2. Dry particle erosion and micro-sandblasting erosion behavior of flame-sprayed PE and PE+25FEP coatings, stainless steel (SS) and PU-paint references.

Erosion test 1: Dry particle erosion				
Sample	Ra_1 (before)	Mass loss (mg)	Ra_2 (after)	Ra_2/Ra_1
FS PE	0.34	-0.011	6.65	19
FS PE+25FEP	0.67	-0.010	7.29	11
SS	0.04	0.031	3.36	88
PU-paint	1.00	-*	-	
Erosion test 2: Micro-sandblasting				
Sample	Ra_1 (before)	Mass loss (mg)	Ra_2 (after)	Ra_2/Ra_1
FS PE	0.34	-0.105	3.27	10
FS PE+25FEP	0.67	-0.085	3.55	5
SS	0.04	0.160	1.23	32
PU-paint	1.00	-*	-	

*Worn out during the test

Stainless steel surfaces eroded with a slight mass loss whereas flame-sprayed PE and PE+25FEP coatings slightly increased their mass in both erosion tests. Flame-sprayed polymer coatings are softer and therefore, erosive particles impinged into the surfaces. Impingement of the erosive particles is illustrated in Fig. 6.

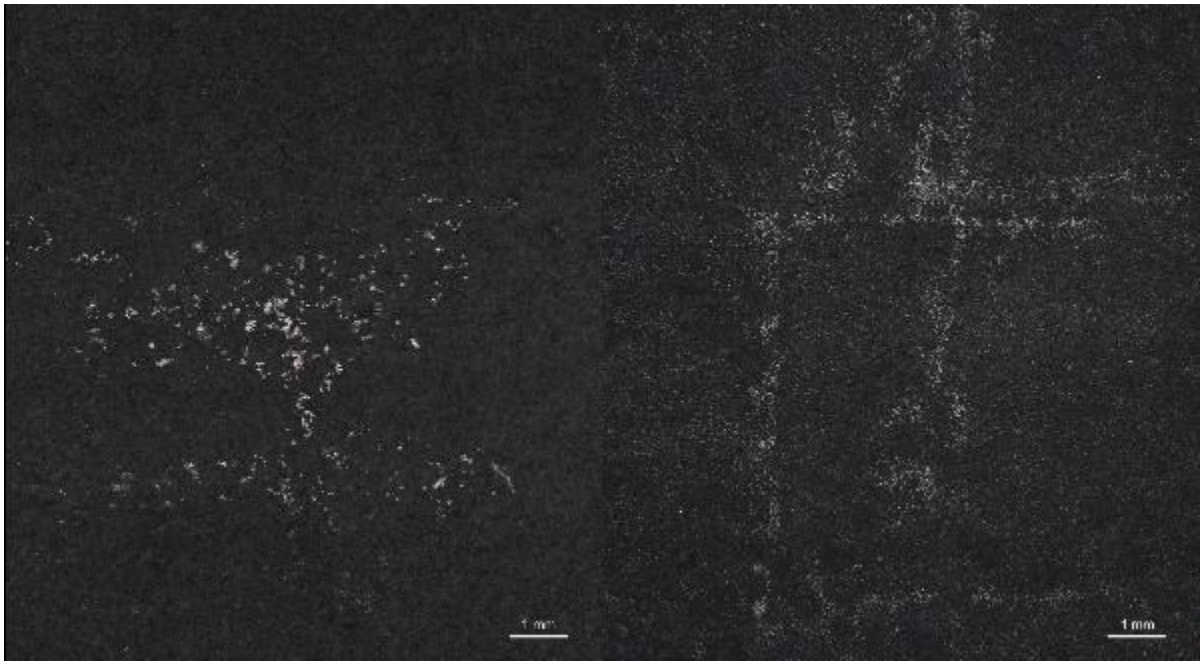

Figure 6. Illustrations of the impingement of erosive particles on flame-sprayed PE coatings a) after Erosion test 1 and b) Erosion test 2. Light grey color on the asperities indicates particle impingement on the PE coating surfaces. Optical microscope images.

The coatings showed durability without erosion. However, the surfaces need to be optimized in order to avoid sand particle impingement in the future. Lima et al. (Ref. 16) have reported good corrosion behavior and wear properties against abrasive wear for flame-sprayed engineering polymer (PEI, PEEK, PA) coatings. The mass loss of stainless steel and the mass gain of flame-sprayed polymer coatings were higher in Erosion test 2 due to the test setup (distance and pressure). Common for both erosion tests was that surface roughness (Ra-values) increased during the test. Roughness changes were higher in Erosion test 1 due to the larger erosive size. However, the roughness ratio (Ra_2/Ra_1) of stainless steel was higher than that of flame-sprayed polymer coatings due to the different type of wear behavior of the surfaces (softer vs. harder and/or elasticity vs. plasticity).

3.3.2 High Velocity Impact Behavior

Besides the anti-icing behavior and wear resistance, impact resistance is expected from polymeric coatings as well. Impacts can be classified into three different categories based on their projectile velocities; low velocity impacts (<11 m/s), high velocity impacts (>11 m/s) and ballistic impacts (>500 m/s) (Ref. 36). Coatings encounter different types of impacts that originate from different sources during

their operating lifetime. Low velocity impacts are caused e.g., in maintenance and high velocity impacts can be associated to impacts that occur in an operating environment. (Ref. 24) Therefore, also high velocity impact behavior was evaluated. This high velocity impact test setup has been successfully used for studying the impact behavior of different materials such as steels (Ref. 25), hybrids (Refs. 24,28), thermally sprayed metal-matrix composite coatings (Ref. 37), thermally sprayed ceramic coatings (Ref. 27) and rubbers (Ref. 38). In the present research, it was used to study the behavior of flame-sprayed polymer coatings. The test results are shown in Table 3.

Table 3. High velocity impact test results. Impact energies, dissipated energies and impact crater dimensions are averages of three parallel samples. FS stands for flame spray and RT for room temperature.

Sample	Temperature	Impact energy (J)	Dissipated energy (J)	Impact crater	
				length (mm)	depth (µm)
FS PE	RT	0.64	0.36	3.32	649
FS PE	-10 °C	0.64	0.26	2.97	384
FS PE+25FEP	RT	0.64	0.39	3.29	728
FS PE+25FEP	-10 °C	0.64	0.28	2.93	482
PU-paint	RT	0.64	Coating failure		
PU-paint	-10 °C	0.64	Coating failure		
Stainless Steel	RT	0.64	0.29	1.76	157
Stainless Steel	-10 °C	0.64	0.27	1.75	129

High velocity impact results presented in Table 3 show the good impact energy absorption capabilities for flame-sprayed PE and PE+25FEP coatings. When the impact results conducted in the room temperature are compared, it can be concluded that flame-sprayed PE and PE+25FEP have significantly higher dissipated energy values compared to stainless steel. However, the impact behavior of flame-sprayed polymer coatings greatly changed at -10 °C. Crater depth for flame-sprayed PE and FS+25FEP coatings at -10 °C is almost half lower in comparison to crater depths at room temperature. This difference in crater depths is presented in Fig. 7, where 3D-optical profiles of impact craters for flame-sprayed PE coatings at room temperature (Fig. 7a) and -10°C (Fig. 7b) are illustrated.

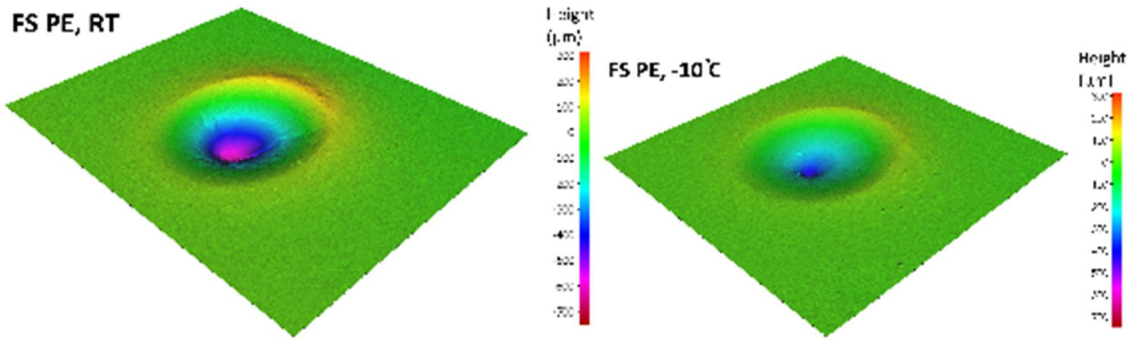

Figure 7. 3D-optical profiles of impact craters of flame-sprayed PE coatings after high velocity impact test at a) room temperature (RT) and b) -10 °C.

Surprisingly, the dissipated energy values of flame-sprayed PE and PE+25FEP coatings at -10 °C are on the same level with the stainless steel (SS). Sayer et al. (Ref. 39) have obtained similar results for carbon-glass composites. They concluded that absorption capability of these composites decreased when the temperature decreased. On the contrary, energy absorption capability increased when temperature increased. (Ref. 39) Sarlin et al. (Ref. 28) have also found that increasing temperature increased the absorbed energy of steel/rubber/composite hybrids.

From a deformation point of view, flame-sprayed PE and PE+25FEP coatings behave structurally similar. Both of these coatings have good resistance against high velocity impacts. This is illustrated in Fig. 8a which shows an impact crater of the flame-sprayed PE coating. However, high velocity impacts produced small subsurface cracks located both near the impact crater and also close to the substrate-coating interface. Figures 8b and 8c illustrate these subsurface cracks formed to flame-sprayed PE+FEP coatings.

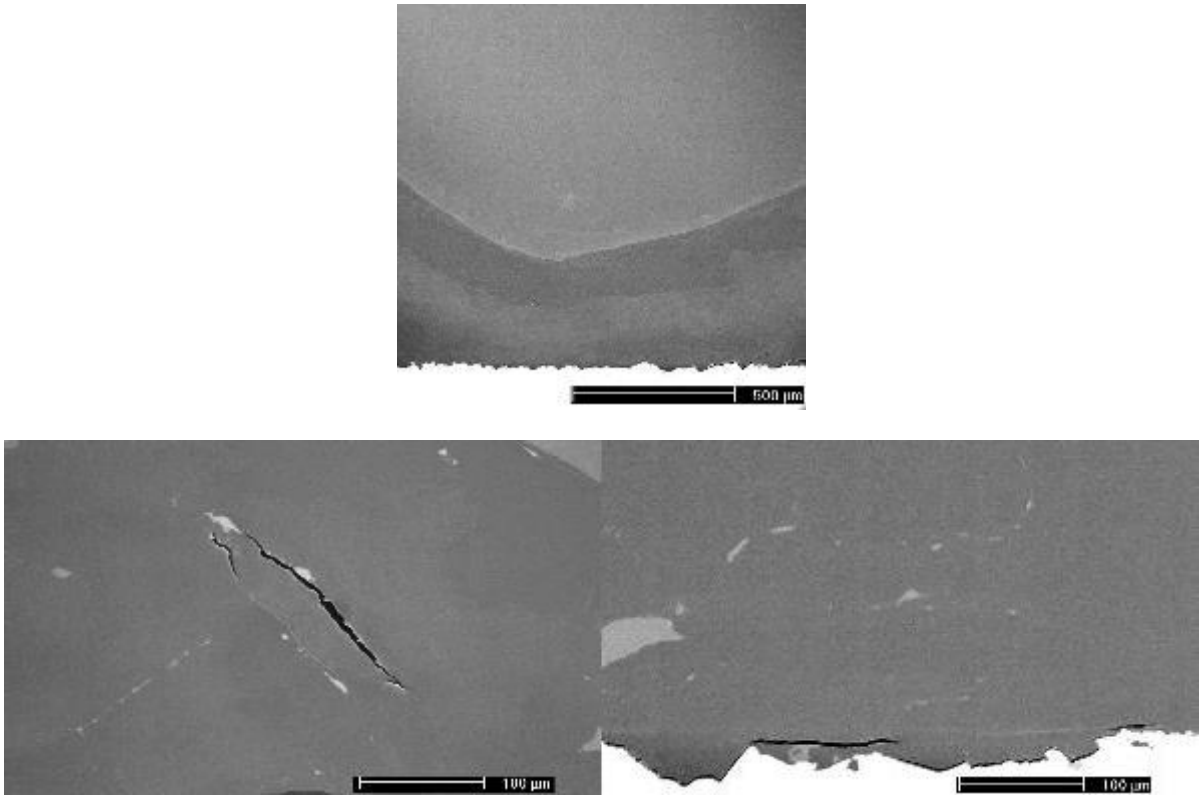

Figure 8. Cross-sections of impact craters after high velocity impact test a) impact crater of flame-sprayed PE coating, b) subsurface crack close to the impact crater of flame-sprayed PE+25FEP coating and c) subsurface crack close to coating-substrate interface of PE+25FEP coating. SEM/SE images.

Regardless of the subsurface cracks, flame-sprayed PE and PE+25FEP coatings can withstand the high velocity impacts with only small structural damage whereas the PU-paint surfaces suffered catastrophic damage. PU-paint surfaces were destroyed and the PU-paint layer delaminated during the test. Difference in elastic properties is causing the different behavior between PU-paint and flame-sprayed PE-based coatings.

4. Conclusions

This study focused on the anti-icing behavior of flame-sprayed PE-based polymer coatings. Icing can cause substantial problems for different industrial fields by decreasing the efficiency, safety and usability of operations. Therefore, new methods of preventing ice accretion on the surfaces or to diminish ice adhesion are welcome. Flame-sprayed PE and PE+25FEP coatings have shown low ice adhesion values compared with stainless steel and aluminum metal surfaces indicating their potential to act as

anti-icing surfaces. Low ice adhesion strengths reflect good anti-icing behavior. Polished flame-sprayed PE and PE+FEP coatings had lower ice adhesion values compared with corresponding as-sprayed coatings which indicate the effect of surface roughness together with wetting behavior (polished surfaces had hydrophobic and as-sprayed surfaces hydrophilic wetting behavior) on icing behavior. Flame-sprayed PE and PE+FEP coatings outperformed PU-paints in the high-velocity impact test. Energy absorption capabilities of flame-sprayed PE and PE+FEP coatings were observed to be temperature dependent; absorbed energy decreased with decreasing temperature in the high-velocity impact tests. Future research will be focused on improving the coating performance in erosive conditions by avoiding erosive impingement without losing anti-icing properties.

5. Acknowledgements

The authors would like to thank M.Sc Henna Niemelä-Anttonen, of Tampere University of Technology, Department of Materials Science, for helping with the ice testing. The research was done partly in the frame of Hydrobond project (EU, FP7, NMP3-SL-20012-3100531).

6. References

[1] C. Stenroos, Properties of icephobic surfaces in different icing conditions, Master Thesis, Tampere University of Technology, Tampere, Finland, 2015, 108 p.

[2] M. Farzaneh, Atmospheric icing of power networks. Springer, London, UK, 2008, 381 p.

[3] A. Kraj, E. Bibeau, Phases of icing on wind turbine blades characterized by ice accumulation, Renewable Energy 35 (5), 2010, p. 966-972.

[4] S. Fikke, J. Kristjánsson, B. Kringlebotn Nygaard, Modern meteorology and atmospheric icing, Atmospheric Icing of Power Networks, IWAIS XI, Montreal, Canada, 2005, p. 1-29.

[5] C. Antonini, Superhydrophobicity as a strategy against icing: Analysis of the water/surface dynamic interaction for icing mitigation. Doctoral Thesis, Università degli studi di Bergamo, 2011, 238 p.

[6] A. Safaee, Nanostructured metal surfaces and their passivation for superhydrophoic and anti-icing applications, Doctoral Thesis, Université du Québec, 2008,182 p.

[7] L. Makkonen, Ice Adhesion -Theory, Measurements and Countermeasures, Journal of Adhesion Science and Technology 26, 2012, p. 413-445.

[8] G. Fortin, J. Perron, Ice Adhesion Models to Predict Shear Stress at Shedding, Journal of Adhesion Science and Technology, 26 (4-5), 2012, p. 523-553.

[9] L. Cao, LA. Jones, V. Sikka, J. Wu, D. Gao, Anti-Icing Superhydrophobic Coatings, Langmuir, 25 (21), 2009, p. 1244-1248.

[10] C.C. Ryerson, Assessment of Superstructure Ice Protection as Applied to Offshore Oil Operations Safety, ERDC/CRREL TR-09-4, 2009, p. 344.

[11] P. Kim, T.-S. Wong, J. Alvarenga, M.J. Kreder, W.E. Adorno-Martinez, J. Aizenberg, Liquid-Infused Nanostructured Surfaces with Extreme Anti-Ice and Anti-Frost Performance, ACS Nano 6 (8), 2012, p. 6569-6577.

[12] S. Jung, M. Dorrestijn, D. Raps, A. Das, C.M. Megaridis, D. Poulikakos, Are Superhydrophobic Surfaces Best for Icephobicity?, Langmuir, 27, 2011, p. 3059-3066.

[13] C.C. Ryerson, Ice protection of offshore platforms, Cold Regions Science and Technology, 65, 2011, p. 97-110.

[14] R. Winkler, R., F. Bűltmann, S. Hartmann, A. Jerz, Thermal Spraying of Polymers: Spraying Processes, Materials and New Trends, Thermal Spray 2003: Advancing the Science & Applying the Technology, C. Moreau, B. Marple (Eds.), ASM International, Ohio, USA, 2003, p. 1635-1638.

[15] E. Petrovicova, L.S. Schadler, Thermal spraying of polymers, International Materials Reviews, 47 (4, 22), 2002, p. 169-190.

[16] C. Lima, N. de Souza, F. Camargo, Study of wear and corrosion performance of thermal sprayed engineering polymers, Surface & Coatings Technology, 220, 2013, p. 140-143.

[17] P. Vuoristo, E. Leivo, E. Turunen, M. Leino, P. Järvelä, T. Mäntylä: Evaluation of Thermally Sprayed and Other Polymeric Coatings for Use in Natural Gas Pipeline Components, Thermal Spray 2003: Advancing the Science & Applying the Technology, C. Moreau, B. Marple (Eds.), ASM International, Ohio, USA, 2003, p. 1693-1702.

[18] D.T. Gawne, Y. Bao, T. Zhang, Influence of Polymer Composition on The Deposition of UHMWPE Coatings, Thermal Spray 2003: Advancing the Science & Applying the Technology, C. Moreau, B. Marple (Eds.), ASM International, Ohio, USA, 2003, p. 1639-1644.

[19] E. Leivo, T. Wilenius, T. Kinos, P. Vuoristo, T. Mäntylä, Properties of thermally sprayed fluoropolymer PVDF, ECTFE, PFA and FEP coatings, Progress in Organic Coatings, 49, 2004, p. 69-73.

[20] S. Yang, Q. Xia, L. Zhu, J. Xue, Q. Wang, Q. Chen, Research on the icephobic properties of fluoropolymer-based materials, Applied Surface Science 257, (1), 2011, p. 4956-4962.

[21] H. Koivuluoto, C. Stenroos, R. Ruohomaa, G. Bolelli, L. Lusvarghi, P. Vuoristo, Research on icing behavior and ice adhesion testing of icephobic surfaces, IWAIS XVI, June 28-July 3, 2015, Uppsala, Sweden, 6 p.

[22] C. Laforte and A. Beisswenger, Icephobic Material Centrifuge Adhesion Test, IWAIS XI, June, 2005, Montreal, Canada, 5 p.

[23] M. Apostol, V.-T. Kuokkala, A. Laukkanen, K. Holmberg, R. Waudby, M. Lindroos, High velocity particle impactor – modeling and experimental verification of impact wear test, World tribology congress, WTC 2013, Sept 8–13, 2013, Turin, Italy

[24] E. Sarlin, M. Apostol, M. Lindroos, V.-T. Kuokkala, J. Vuorinen, T. Lepistö, M. Vippola, Impact properties of novel corrosion resistant hybrid structures. Composite Structures, 108, 2014, p. 886–893

[25] M. Lindroos, M. Apostol, V. Kuokkala, A. Laukkanen, K. Valtonen, K. Holmberg, O. Oja, Experimental study on the behavior of wear resistant steels under high velocity single particle impacts, International Journal of Impact Engineering, 78, 2015, p. 114-127.

[26] M. Lindroos, V. Ratia, M. Apostol, K. Valtonen, A. Laukkanen, W. Molnar, K. Holmberg, V.-T. Kuokkala, The effect of impact conditions on the wear and deformation behavior of wear resistant steels, Wear, 328-329, 2015, p. 197–205.

[27] J. Kiilakoski, M. Lindroos, M. Apostol, H. Koivuluoto, V-T. Kuokkala, P. Vuoristo, Characterization of High-Velocity Single Particle Impacts on Plasma-Sprayed Ceramic Coatings, Journal of Thermal Spray Technology, 25 (6), 2016, 1127-1137.

[28] E. Sarlin, M. Lindroos, M. Apostol, V-T. Kuokkala, J. Vuorinen, T. Lepistö, M. Vilppola, The effect of test parameters on the impact resistance of a stainless steel/rubber/composite hybrid structure. Composite structures, 113, 2014, p. 469-475.

[29] M. Zou, S. Beckford, R. Wei, C. Ellis, G. Hatton M. Miller, Effects of surface roughness and energy on ice adhesion strength, Applied Surface Science, 257 (8), 2011, p. 3786-3792.

[30] M. Susoff, K. Siegmann, C. Pfaffenroth, M. Hirayama, Evaluation of icephobic coatings - Screening of different coatings and influence of roughness, Applied Surface Science, 282, 2013, p. 870-879.

[31] T. Bharathidasan, S. Kumar, M. Bobji, R. Chakradhar, B. Basu, Effect of wettability and surface roughness on ice-adhesion strength of hydrophilic, hydrophobic and superhydrophobic surfaces, Applied Surface Science, 314, 2014, p. 241-250.

[32] R. Menini, M. Farzaneh, Elaboration of Al_2O_3/PTFE icephobic coatings for protecting aluminum surfaces, Surface and Coatings Technology, 203 (14), 2009, p. 1941-1946.

[33] S. Farhadi, M. Farzaneh, S. A. Kulinich, Anti-icing performance of superhydrophobic surfaces, Applied Surface Science, 257 (14), 2011, p. 6264-6269.

[34] S. A. Kulinich, S. Farhadi, K. Nose, X. W. Du, Superhydrophobic surfaces: are they really ice-repellent?, Langmuir, 27 (1), 2011, p. 25-29.

[35] H. Dodiuk, S. Kenig, A. Dotan, Do Self-cleaning Surfaces Repel Ice?, Journal of Adhesion Science and Technology, 26 (4-5), 2012, p. 701-714.

[36] M. Hagenbeek, Impact properties, A. Vlot, J.W. Gunnink (Eds.), Fibre metal laminates: an introduction, Kluwer Academic Publishers, Dordrecht, 2001, p. 409–426

[37] R. Waudby, T. Varis, T. Suhonen, K. Holmberg, M. Apostol, M. Lindroos, V. Kuokkala, High velocity impact testing of thermal spray hard carbide coatings on steel substrates, 5th World Tribology Congress, WTC 2013, 2013, p. 3–6.

[38] W. Molnar, S. Nugent, M. Lindroos, M. Apostol, M. Varga, Ballistic and numerical simulation of impacting goods on conveyor belt rubber, Polymer Testing, 42, 2015, p. 1–7.

[39] M. Sayer, N.B. Bektaş, E. Demir, H. Çallioğlu, The effect of temperatures on hybrid composite laminates under impact loading, Composites Part B: Engineering, 43 (5), 2012, p. 2152-2160.